



ELSEVIER

Available online at [www.sciencedirect.com](http://www.sciencedirect.com)

ScienceDirect

journal homepage: [www.intl.elsevierhealth.com/journals/dema](http://www.intl.elsevierhealth.com/journals/dema)

# Physical properties and cytotoxicity of antimicrobial dental resin adhesives containing dimethacrylate oligomers of Ciprofloxacin and Metronidazole

Yasaman Delaviz<sup>a</sup>, Timothy W. Liu<sup>a</sup>, Ashley R. Deonarain<sup>b</sup>, Yoav Finer<sup>a,c</sup>, Babak Shokati<sup>c</sup>, J. Paul Santerre<sup>a,c,\*</sup>

<sup>a</sup> Institute of Biomaterials and Biomedical Engineering, University of Toronto, Ontario, Canada

<sup>b</sup> Division of Engineering Science, University of Toronto, Ontario, Canada

<sup>c</sup> Faculty of Dentistry, University of Toronto, Ontario, Canada

## ARTICLE INFO

### Article history:

Received 19 May 2018

Received in revised form

14 October 2018

Accepted 14 November 2018

### Keywords:

Resin composites

*Streptococcus mutans*

Interfacial fracture toughness

Methacrylate

Secondary caries

Esterase

## ABSTRACT

**Objective.** Antimicrobial oligomers synthesized from ciprofloxacin (CF) and metronidazole (MN) were investigated for their potential use in dental adhesives.

**Methods.** Susceptibility of the cariogenic bacterium *Streptococcus mutans* UA159 to CF, MN, and CF/MN combination was evaluated. Hydrolytic stability and drug release from the oligomers was studied in buffer and simulated human salivary esterase conditions. Cytotoxicity of films with 15 wt% drug oligomers co-polymerized with commercial monomers were assessed using human gingival fibroblasts (HGFs). In-house adhesives were prepared and characterized for viscosity. Polymerized films were analysed for gel content and water swelling. Interfacial fracture toughness ( $K_{IC}$ ) of composites bonded to dentin by either a 2 or 3-step etch-and-rinse approach using the in-house formulated adhesives was measured.

**Results.** The respective minimum inhibitory concentration for CF and MN against *S. mutans* was 0.7 and 2400  $\mu\text{g/mL}$ , with the combination having an additive effect (0.35  $\mu\text{g/mL}$  CF with 1200  $\mu\text{g/mL}$  MN). Antibiotics were released upon hydrolysis of the oligomers. Films containing the drug oligomers were not cytotoxic against HGFs. Replacing 2-hydroxyethyl methacrylate with the drug oligomers increased the viscosity of the experimental adhesives, reduced gel content, and decreased swelling of films in water. Antimicrobial adhesives demonstrated bonding to dentin with interfacial  $K_{IC}$  values comparable to the in-house control in the 2-step application, and with slightly lower  $K_{IC}$  values in the 3-step approach. **Significance.** The antimicrobial oligomers can be incorporated into dental adhesive systems using formulations that show comparable fracture toughness to commercial materials, and may provide a means to deliver local antimicrobial drug release at the marginal interface.

© 2018 The Academy of Dental Materials. Published by Elsevier Inc. All rights reserved.

\* Corresponding author at: Faculty of Dentistry and Institute of Biomaterials and Biomedical Engineering, University of Toronto, Ted Rogers Centre for Heart Research, 661 University Ave, Mars West Tower, 14th Floor, Toronto, Ontario, M5G 1M1, Canada.

E-mail address: [paul.santerre@dentistry.utoronto.ca](mailto:paul.santerre@dentistry.utoronto.ca) (J.P. Santerre).

<https://doi.org/10.1016/j.dental.2018.11.016>

0109-5641/© 2018 The Academy of Dental Materials. Published by Elsevier Inc. All rights reserved.

## 1. Introduction

Resin composites are the most widely used dental restorative material [1]. Resin composites are bonded to teeth using adhesive systems, which seal the interface by replacing some of the inorganic tooth component with resin monomers. The latter bond by mechanically interlocking into the tooth structure upon polymerization [2]. Two main types of adhesive systems used commercially are the etch-and-rinse (E&R) systems, also known as total etch, which remove the smear layer (a thin layer of debris remaining on the tooth surface after dental instrumentation procedures) and the self-etch adhesive systems that modify the smear layer by incorporating resin into the demineralized dentin substrate [3]. E&R adhesive systems are the gold standard [4], offered in two- or three-step application workflows. This technique involves the application of an acidic etchant that demineralizes the tooth and generates porous features that enable the mechanical interlocking of the resin into the enamel etch-pits, and allows for improved integration of resin with the exposed collagen lattice in the dentin [2]. In 2-step E&R systems, after etching, an adhesive composed of solvent and resin is applied to the tooth structure and photo-polymerized. Some systems require repeating this step once the solvent in the applied adhesive solution has evaporated, resulting in the first layer effectively acting as a primer and the second layer as the adhesive layer [5]. In a 3-step E&R application, after etching, a dedicated primer composed of solvent and resin is applied to the tooth without polymerization, followed by the application of the more viscous adhesive that is photo-polymerized.

Commercial adhesive systems typically use methacrylate monomers to achieve rapid photo-polymerization of the resin. However, the methacrylate moiety introduces hydrolytically susceptible chemistries that render the resin vulnerable to esterolytic hydrolysis, enabled in the oral cavity by enzymes [6–9]. This facilitates marginal breakdown between the tooth and restorative material [7]. The micro-leakage of oral bacteria and salivary enzymes into these gaps generates a cariogenic environment that challenges the adhesive-tooth interface [7,10]. A recent review published, which included 25 studies and provided information on 49,704 restoration replacements, has reported secondary caries (recurrent caries at the tooth and restoration interface) as the main reason for up to 59% of restorations replaced [11]. Therefore, there is a need for innovative adhesives that have greater resistance against degradation, but also provide long-term antimicrobial properties that could control bacterial growth around and within the margins, while still achieving rapid curing of methacrylate monomers.

To attain short-term antibacterial properties, previous studies have investigated the release of antimicrobial agents such as chlorhexidine [12], metallic oxides [13], and antibiotics [14] from restorative materials. With a variety of bacteria involved in caries development, the latter study looked at the release of ciprofloxacin (CF) and metronidazole (MN) along with Cefaclor from glass ionomer cements (GICs). The use of antibiotics in long-term applications continue to be a matter of debate in the scientific community. The emergence of resistance bacterial strain is a clinical concern with exten-

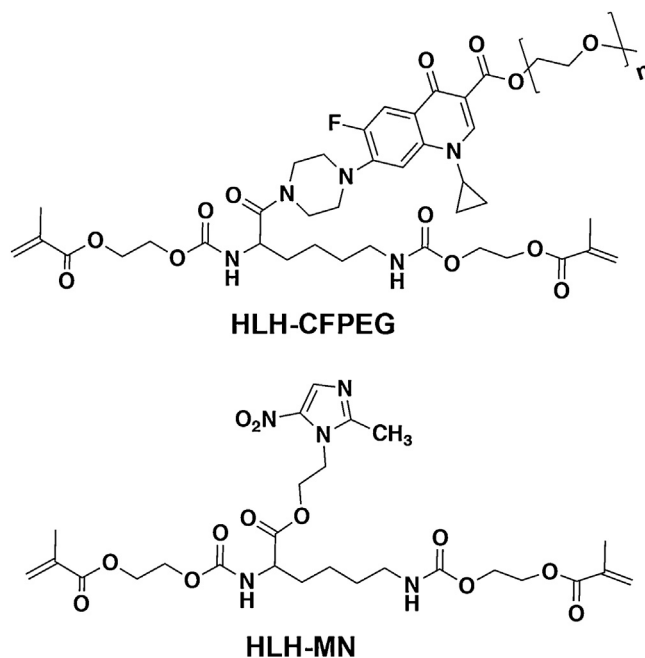


**Fig 1 – Chemical structures for HEMA/lysine/HEMA-CF/polyethylene glycol (HLH-CFPEG) [18] and HEMA/lysine/HEMA-MN (HLH-MN).**

sive use or misuse of antibiotics, which may occur through mechanisms such as inactivation of the drug, modification of the site of action, modification of the cell walls permeability, and overproduction of the target enzyme [15]. Concerns of bacterial resistance has led to new strategies being explored that circumvent resistance with long-term use of antibiotics. Targeted local delivery of antibiotics from medical devices is one example of the many strategies currently being studied to minimize the systematic side effects of long-term exposure to antibiotics [16]. Combination therapies have also been widely used to increase the spectrum of activity, reduce the likelihood of bacterial resistance, and potentially create cooperative pathways with one agent enhancing the activity of another antibiotic [17], by compromising the bacterial function via one pathway and simultaneously rendering it more vulnerable to the second pathway. Therefore, there is a good rationale to explore the value of multiple types of antibiotic resin oligomers in developing antimicrobial adhesive systems.

One strategy for long-term effective kill of bacteria migrating into the restoration-tooth marginal interface is the release of agents as degradation by-products from some element of the resin adhesive at the interface. Recent work has reported on the synthesis of an antimicrobial oligomer that releases CF upon hydrolytic degradation [18]. The oligomer is composed of a dimethacrylate backbone of 2-hydroxyethyl methacrylate (HEMA) and lysine with a pegylated CF chain coupled in pendent (referred to as HLH-CFPEG, Fig. 1). The urethane groups generated in the dimethacrylate backbone have the potential to hydrogen bond with the ester moieties, which can reduce hydrolysis [19]. In the present study, MN was covalently coupled to the same dimethacrylate backbone in order to yield a newly synthesized oligomer (HLH-MN,

Fig. 1). It should be noted that HLH-MN is a monodisperse oligomer but HLH-CFPEG is a polydisperse oligomer because of the polydisperse polyethylene glycol (PEG) chain coupled in pendant, which was added to provide diluent properties to HLH-CFPEG. For greater chain mobility and lower viscosity, a branched structure was also used to reduce the tendency of CF molecules to self-assemble and aggregate through pi-pi bonding between the aromatic groups in their pre-polymerized state [18]. Methacrylate- and acrylate-based monomers have been previously synthesized using CF [20] and MN [21], respectively. The corresponding polymers have demonstrated antimicrobial activity against the tested microorganisms. These monomers however generate linear polymers while dimethacrylate oligomers generate cross-linked systems that are preferred for reinforcing the adhesive resin [2]. Therefore, the objective of the current work was to investigate the integration of both HLH-CFPEG and HLH-MN together into dental adhesive polymers and to compare them to the character of their respective mono-drug oligomers and related cured resins. The new adhesive resins were compared to in-house formulated controls for cytotoxicity character, gel content, and bonding to dentin under simulated wet oral conditions when used in an E&R adhesive system.

## 2. Materials and methods

Reagents were purchased from Sigma-Aldrich (St. Louis, MO, United States) unless otherwise stated.

### 2.1. Antibiotic susceptibility assessment

*Streptococcus mutans* UA159 stored in 20% glycerol broth at  $-80^{\circ}\text{C}$  was recovered and sub-cultured on Todd–Hewitt yeast extract (THYE) agar. Overnight cultures were prepared and grown in THYE broth (BioShop, Burlington, ON, Canada) [18]. The overnights were diluted 1:10 in fresh THYE, grown to mid-logarithmic phase (optical density at 600 nm [ $\text{OD}_{600}$ ] of  $\sim 0.4$ ), and cell count adjusted to  $\sim 10^6$  colony forming units (CFU) per mL using fresh broth. The minimum inhibitory concentrations (MIC) were determined after incubating 100  $\mu\text{L}$  of suspension ( $\sim 10^6$  CFU/mL at mid-log) with 100  $\mu\text{L}$  antibiotic solution overnight at  $37^{\circ}\text{C}$  and 5%  $\text{CO}_2$ . The antibiotic dilutions were prepared in ultrapure water using CF-HCl (Alfa Aesar, Ward Hill, MA, USA) and MN. Negative and positive controls were included by adding 100  $\mu\text{L}$  of water with 100  $\mu\text{L}$  of THYE broth or inoculums, respectively. MIC was recorded as the lowest concentration of antibiotic that inhibited visible growth of bacteria after 18 h of incubation. After MIC recording,  $\text{OD}_{600}$  were read by a plate reader (VersaMax™ tunable, Molecular Devices Corporation, Sunnyvale, CA, USA). The percentage (%) of bacterial growth was then calculated using the following equation:

$$\% \text{ Bacterial growth} = \left( \frac{\text{OD}_{600\text{nm}} \text{ of sample} - \text{OD}_{600\text{nm}} \text{ media}}{\text{OD}_{600\text{nm}} \text{ of control} - \text{OD}_{600\text{nm}} \text{ media}} \right) \times 100$$

The cooperative interaction between CF and MN was assessed by calculating the fractional inhibitory concentration (FIC) index (FICI), a mathematical expression used to predict synergy [22]. The interaction was classified as synergistic

( $\text{FICI} \leq 0.5$ ), additive ( $0.5 < \text{FICI} \leq 1$ ), or indifferent ( $1 > \text{FICI} \leq 2$ ) [23]. The FICI was calculated from MICs using the equations:

$$\text{FICI} = \text{FIC}_{\text{CF}} + \text{FIC}_{\text{MN}} = \frac{[\text{MIC}_{\text{CF+MN}}]}{[\text{MIC}_{\text{CF}}]} + \frac{[\text{MIC}_{\text{CF+MN}}]}{[\text{MIC}_{\text{MN}}]}$$

In a separate experiment, % viability of *S. mutans* was determined for CF and the combination with MN. Antibiotic dilutions were prepared using CF-HCl and MN first dissolved in ultrapure water and further diluted with Dulbecco's phosphate buffered saline (DPBS; Gibco, Grand Island, NY, USA). To a 96-well plate in the laminar flow hood, 100  $\mu\text{L}$  of suspension ( $\sim 10^6$  CFU/mL at mid-log) was added with either 100  $\mu\text{L}$  of antibiotic solution or 100  $\mu\text{L}$  of DPBS (negative control). Sterility controls were included, containing 100  $\mu\text{L}$  DPBS with 100  $\mu\text{L}$  THYE broth. After overnight incubation at  $37^{\circ}\text{C}$  and 5%  $\text{CO}_2$ , wells were serially diluted with DPBS, plated onto THYE agar plates and incubated for 48 h ( $37^{\circ}\text{C}$ , 5%  $\text{CO}_2$ ). Formed colonies were counted and % viability was calculated by normalizing to the no drug control.

### 2.2. Antimicrobial oligomer synthesis

The dimethacrylate backbone was synthesized as described previously [18]. Using carbodiimide chemistry, MN was coupled to the pendant carboxylic acid moiety of the lysine-HEMA dimethacrylate backbone, labelled as product 2 in supplementary Fig. S1. MN (2 g, 11.7 mmol), product 2 (5.36 g, 11.7 mmol), 1-ethyl-3-[3-dimethylaminopropyl] carbodiimide hydrochloride (Advanced ChemTech CreoSalus, Louisville, Kentucky, USA) (EDC-HCl; 20.1 g, 105.2 mmol), and 4-(dimethylamino) pyridine (DMAP; 0.7 g, 5.8 mmol) were dissolved in anhydrous chloroform (350 mL) and sealed under nitrogen, with 4-methoxyphenol ( $\sim 10$  mg) added as inhibitor and triethylamine (10 mL) added to facilitate with MN dissolution. The reaction components were stirred for 7 days at room temperature and covered with aluminum foil. The base was then neutralized by adding 10 mL of 1N hydrochloric acid (HCl; BioShop, Burlington, ON, Canada) to 30 mL of reaction mixture in a Falcon tube. The mixture was vortexed, centrifuged for 10 min at 3000 rpm, and the organic phase was collected and washed two more times. Any carried over salt and EDC in the organic phase was subsequently extracted with water ( $\times 3$ ). The solvent was removed by rotary evaporation, and HLH-MN was isolated and stored at  $-20^{\circ}\text{C}$ .

### 2.3. Characterization of synthesized oligomers

The characterization of HLH-CFPEG was previously reported on [18]. The structure of HLH-MN and associated precursors were characterized by proton nuclear magnetic resonance spectroscopy ( $^1\text{H-NMR}$ ) using a Varian Mercury 400 MHz spectrometer (Department of Chemistry, University of Toronto).  $^1\text{H-NMR}$  was run in deuterated chloroform with 0.05 v/v TMS ( $\text{CDCl}_3$ ; Cambridge Isotope Laboratories, MA, USA). The molecular weight was determined by Electron Spray Ionization Mass Spectrometry (ESI-MS) at the Translational Biology and Engineering Program (TBEP) facility, at the University of Toronto.

#### 2.4. Cured adhesive resin film preparation

Films for the different resin formulations were prepared using the commercial monomers bisphenol A diglycidylmethacrylate (BisGMA; Esschem, Linwood, PA, USA) and HEMA combined with the antimicrobial oligomers. Resin mixtures were prepared with the four monomers (wt%): HLH-CFPEG: HLH-MN: BisGMA: HEMA. A formulation of 0:0:55:45 was used as the control. Unreacted mixtures (containing 1 g of monomer and 64  $\mu$ L of initiator solution) were prepared and photo-polymerized as described previously [18]. The initiator solution consisted of 0.2 g of camphorquinone (CQ) and 0.4 g 2-(dimethylamino)ethyl methacrylate (DMAEM) in 3.6 mL of anhydrous dichloromethane. Films were prepared on glass slides for contact angle measurements and in polytetrafluoroethylene (PTFE) moulds using polyester (Mylar™) strips for cytotoxicity and biodegradation analysis. The mixture was left to air dry on the glass slides or in the PTFE mould at room temperature (while kept shielded from light) for 15 min prior to being photo-polymerized for 60 s from each side using a photocuring light source (either a FLASHlite 2.0 or Sapphire plus, (DenMat, Santa Maria CA, USA)). Consistent light intensity was verified by the built-in meters. Samples for cytotoxicity and biodegradation studies were post-cured in the oven for 24 h at 55°C–60°C to achieve a best degree of polymerization.

#### 2.5. Biodegradation analysis

Degradation of HLH-MN oligomer was characterized relative to the BisGMA monomer and compared to previously published findings for HLH-CFPEG [18]. Degradation studies were performed in DPBS and simulated human salivary esterase (SHSE) solution containing cholesterol esterase (CE; Toyobo Co. COE-313, Osaka, Japan) and butyrylcholinesterase from equine serum, also known as pseudocholinesterase (PCE; Sigma-Aldrich C7512-6KU), with matching activities to human saliva as previously described [18]. BisGMA and HLH-MN were prepared separately in methanol and added to either DPBS or filtered SHSE solution to yield a final concentration of 0.1 mM with 2 vol% methanol. This concentration of methanol does not affect the enzyme activity [24]. For each time point and condition, three vials containing 1 mL of solution were incubated at 37°C. The CE-activity in SHSE was replenished daily with 10  $\mu$ L of CE solution (0.22  $\mu$ m syringe filtered), as CE but not PCE lost activity over 24 h. The controls were replenished with 10  $\mu$ L of DPBS to maintain similar volume. At specific time points (0–4 days), the corresponding vials were removed and equal volume of methanol was added to denature the protein.

For polymer biodegradation analysis, vials containing 8 cured films (1 mm H  $\times$  3 mm D) of 15 wt% HLH-MN (0:15:55:30) or non-drug control (0:0:55:45) were pre-incubated in 70% ethanol for 48 h to remove potential contaminants from the samples and extract residual traces of unreacted monomer. Samples were dried for 1 h in the biosafety cabinet prior to adding 1 mL of either filtered DPBS or SHSE, and then incubated at 37°C. Enzyme replenishment and sample collection was performed following the protocol described previously [18]. After adding methanol, the collected biodegradation solutions were filtered by Amicon Ultra-0.5 centrifugal filtration units with a 3 kDa molecular weight cut off (Millipore, Bedford,

MA, USA) for 30 min at 14,000 rcs and 8°C. The supernatants were stored at –20°C until analysis.

Test solutions were analyzed using a reversed phase high performance liquid chromatography (HPLC) system (Waters, Mississauga, ON), consisting of a 600E multi-solvent delivery system and a 996-photodiode array detector. Samples were injected into Kinetex™ Phenyl Hexyl column (Phenomenex, Torrance, CA, USA) and eluted using the gradient method phase previously described [18]. The signals from the data acquisition system were processed and peak analysis was performed using the Empower Software (Waters Corporation, Milford, USA). Concentrations were calculated from standard curve equations ( $n=3$ ,  $r^2>0.99$ ) collected at the following elution time and the characteristic wavelength for each compound: MN (6.8 min, 315 nm), bisphenol A bis (2,3-dihydroxypropyl) ether (BisHPPP; 19.8 min, 280 nm), HLH-MN (22.9 min, 315 nm), and BisGMA (25.6 min, 280 nm). The experiments were repeated three times ( $n=9$ ).

#### 2.6. Cytotoxicity assessment against human gingival fibroblasts (HGFs)

HGFs are the most abundant resident cells in gingival connective tissue and are easily cultured in Dulbecco's Modified Eagle's Medium (DMEM; GibcoBRL) [25], and thus were selected as the representative cell type of oral tissue for cytotoxicity assessment. HGFs (ATCC CRL-2014) were cultured at 37°C and 5% CO<sub>2</sub> in DMEM supplemented with 10% fetal bovine serum, 100 U/mL penicillin, and 100  $\mu$ g/mL streptomycin at 37°C and 5% CO<sub>2</sub>. The medium was changed every 2–3 days. HGF cells were trypsinized at 80–90% confluency. Cell metabolic activity and DNA mass quantification were assayed in parallel.

##### 2.6.1. Toxicity of films

Films (1 mm H  $\times$  5 mm D) were prepared as described in section 2.4, with the following formulations, HLH-CFPEG: HLH-MN: BisGMA: HEMA, respectively with wt% ratios of 15:0:55:30, 0:15:55:30, and 0:0:55:45. Two conditions (with and without residual monomers) were set up to assess whether residual monomers are abundant enough to present any cytotoxic effect. Prior to cell culture, films were first treated with 70% ethanol at room temperature for 24 h in a 48-well polystyrene plate. In the no-residual monomer condition, the plate was covered and sealed during extraction of residual monomers by ethanol, and the solution was removed after 24 h and samples were left to air dry for 1 h under a sterile laminar flow condition. In the samples that retained residual monomers, the plate was left uncovered under a sterile laminar flow condition enabling evaporation of the ethanol overnight. Test samples were then conditioned with 250  $\mu$ L of DMEM for 24 h. To each well, 100  $\mu$ L of HGF cell suspension (~50,000 cells/well) was added. Positive control wells were included with 20 vol% DMSO. Cytotoxicity of the polymers were assessed 24 h after seeding. The experiment was repeated three times ( $n=11$  per formulation in total).

##### 2.6.2. Toxicity of resin by-product extracts

For each formulation, 40 films (1 mm H  $\times$  1 mm D; total surface area of 188.4 mm<sup>2</sup>) were pre-incubated in 70% ethanol at room temperature for 48 h, air dried in the biosafety cabinet, and

incubated with 3 mL of sterile DMEM in a sealed glass vial (9 vials per formulation) for 28 days at 37°C. Separate vials with only DMEM were also incubated to serve as an aged media control. Concentration of resin by-product extracts (methacrylic acid (MAA), BisHPPP, CF, and MN) in the DMEM extract solutions were determined by HPLC. To a 96-well tissue culture plate, 200 µL of HGF cell suspension (~20,000 cells/well) were added. After 24 h of incubation, media was aspirated and fresh DMEM was added along with 0, 50, or 90 vol% of the DMEM extract solution. Positive control wells were included with 20 vol% DMSO. Cytotoxicity was then assessed 48 h post-seeding (24 h after addition of test solution). Experiment was repeated three times (n = 9 per formulation).

### 2.6.3. DNA mass quantification

DNA mass quantification was assayed using Hoechst 33258 DNA stain [26]. Briefly, the samples were washed with DPBS and incubated with cell lysis buffer (0.05% Triton X-100 and 50 mM ethylenediaminetetraacetic acid in PBS) for 1 h on ice. The cell lysates were then transferred to a black polypropylene flat-bottom 96-well plate containing the DNA stain and read using a fluorescence microplate reader (Bio-Tek FL600 Instruments, Inc., Winooski, VT, USA) set to an excitation wavelength of 360 nm and emission wavelength of 460 nm. Background fluorescence emitted from the control wells with no cells was subtracted from the readings. The obtained values were compared to a standard curve (calf thymus DNA).

### 2.6.4. Water-soluble tetrazolium (WST)-1 assay

The metabolic activity of HGFs was quantified using a WST-1 assay (Roche Diagnostics, Laval, Quebec, Canada) [27]. Briefly, the media from each well was aspirated and the reagent was added at a ratio of 1:10 (WST-1:DMEM), with 10 µL of WST-1 added to 96-well plates and 17.4 µL to 48-well plates. The plates were incubated at 37°C with 5% CO<sub>2</sub> for 1 h and then read at an absorbance of 450 nm (background reading at 650 nm) using the VersaMax™ tunable microplate reader. Absorbance from the control growth media (GM) wells were subtracted from all readings.

### 2.7. Water contact angle measurements of cured resin films

Contact angle measurements on cured films were obtained by means of a goniometer (NRL C.A. goniometer, Ramé-Hart, Inc., Mountain Lakes, NJ, USA) using established protocols [10]. For each formulation, 3 films were prepared, and 5 measurements were taken per film.

### 2.8. In-house adhesive formulations

In-house adhesive formulations were prepared using (in wt%) 85% resin, 13.8% ethanol, 0.4% CQ, and 0.8% DMAEM. The resin phase of the adhesive contained defined amounts (in wt%) of the four monomers: HLH-CFPEG: HLH-MN: BisGMA: HEMA, with 0:0:55:45 used as a model resin control [28]. The following test formulations were studied: 15:0:55:30; 0:15:55:30; 15:15:55:15; and 20:15:55:10. The prepared resins were mixed by gentle shaking overnight in sealed glass vials covered with aluminium foil.

### 2.9. Gel content and degree of swelling

Cured adhesive films (1 mm H × 3 mm D) were prepared in PTFE moulds with one surface exposed to air during light curing. Using an analytical balance with accuracy of ±0.0001 g (Mettler AT 201, Fisher Scientific, USA), gel content and degree of swelling were determined by gravimetric analysis after 48 h of incubation in dichloromethane and water, respectively [18].

### 2.10. Rheological characterization of the oligomers and formulated adhesives

The viscosity ( $\eta$ ) of the monomers and the formulated uncured adhesive mixtures were measured as a function of shear rate ( $\dot{\gamma}$ ). The rheological data was collected at the University of Toronto in the Shoichet laboratory using a TA Instruments Ar1000 rheometer (New Castle, DE, USA) equipped with a 20 mm, 1° acrylic cone, with gap size of 23 µm. The temperature was maintained at 25°C using an integrated Peltier plate, and sample evaporation was minimized using a solvent trap. The viscosities were evaluated from the recorded shear stress ( $\tau_w$ ) for shear rates ranging between 0.6–600 s<sup>-1</sup> for adhesives and 0.1–100 s<sup>-1</sup> for pure monomers.

$$\eta = \frac{\tau_w}{\dot{\gamma}}$$

### 2.11. Interfacial fracture toughness of restoration-dentin interface

Intact posterior permanent teeth were collected by oral surgeons within the Toronto area (University of Toronto Human ethics protocol #32320) and immediately stored in distilled water at -20°C until use. Miniature short rod (mini-SR) specimens with a bonded resin-dentin interface were prepared as described previously [6,29]. The roots were fixed in resin (Pattern Resin™ LS, GC America Inc., Alsip, Illinois, USA) and then sectioned using a water-cooled low-speed diamond saw (Buehler Ltd, Lake Bluff, IL) to obtain rectangular shape dentin slabs (7 × 3.7 mm with thickness of 0.75 ± 0.05 mm). One side of the exposed dentin was conditioned for ~15 s using phosphoric acid (Etch-Rite™, Pulpdent Corporation, Watertown, MA, USA), then rinsed with water (~10 s), followed by water and air (~5 s), and then air dried for ~2 s. Adhesive (Scotchbond™ Universal adhesive, 3M Co., St. Paul, MN, USA) was then applied to the etched surface and light cured for 20 s (Sapphire plus, DenMat, Santa Maria CA, USA). The slabs were placed into stainless-steel moulds and packed with resin composite (Filtek™ Z250™, 3M Co., St. Paul, MN, USA) and light cured for 30 s per side. Second half of the specimens were prepared by etching the opposing dentinal surface as described above. In the 3-step application, priming agent (Adper™ Scotchbond™ Multi-Purpose primer, 3M Co., St. Paul, MN, USA) was applied to the etched surface followed by a gentle stream of air for ~5 s (this step was skipped in the 2-step approach). In-house experimental resins were then applied to the primed (3-step) or etched (2-step) dentin substrates and light cured for 20 s. The specimens were then inserted into custom PTFE moulds and a stainless-steel spacer was placed over the surface to form a chevron shaped area.

The moulds were filled with Filtek™ Z250™ and light cured for 30 s per side. The mini-SR specimens were then incubated in DPBS containing 500 U/mL penicillin and 500 µg/mL streptomycin for 24 h at room temperature. After incubation, the specimens were placed into a customized jig and loaded at a cross-head speed of 0.5 mm/min on the Instron Universal testing machine (model 4301, Instron®, Norwood, MA, USA) [6,29,30]. The  $K_{IC}$  values were calculated using the following equation, where  $P_C$  is the peak force at fracture,  $Y_m^*$  is the dimensionless stress intensity factor coefficient,  $D$  is the specimen diameter, and  $W$  is the specimen length:

$$K_{IC} = \frac{P_C \times Y_m^*}{D\sqrt{W}}$$

### 2.12. Scanning electron microscopy (SEM) analysis of fractured surfaces

Fractured mini-SR samples were dehydrated by soaking in increasing concentrations of ethanol (30%, 50%, 75%) for 1 h, followed by overnight incubation in 90% ethanol. The samples were then incubated in 100% ethanol for 1 h, critically point dried, mounted onto aluminium stubs, and sputter coated with platinum using an SC515 SEC Coating Unit (Polaron Equipment, Uckfield, UK). Fractured surfaces were imaged ( $\times 1000$  magnification) at a voltage of 10 kV by SEM (Hitachi S2500 SEM, Mito City, Japan) at the Faculty of Dentistry, University of Toronto.

### 2.13. Solvent evaporation during light curing of adhesives

To a petri dish, 20 µL of adhesive was added and the mass was recorded before and after light curing for 20 s. The extent of solvent evaporation was determined by gravimetric analysis using an analytical balance with an accuracy of  $\pm 0.0001$  g. This was done by taking the difference in mass right after 20 s of light curing and dividing it by the initial mass prior to curing.

### 2.14. Statistical analysis

Statistical analysis was performed using the IBM SPSS program v20.0 (IBM Corp., Armonk, NY, USA). Levene's test for homogeneity of the variances and Shapiro–Wilk's test for normality were first conducted. Mean comparisons between groups were made using one-way analysis of variance (ANOVA) with Tukey's honest significant difference (HSD) post-hoc analysis to determine differences in  $K_{IC}$ , % cellularity, WST-1 absorbance, solvent evaporation during curing, contact angle, water swelling, and % of filled tubules in the 2-step application. Welch's ANOVA with Dunnett's T3 post-hoc analysis was used in the event of unequal variance (i.e. cytotoxicity of resin extracts and films without residual monomer, gel content, and % of filled tubules in the 3-step approach). Student's t-test was used to determine differences in % of filled tubules in the 2-step vs. 3-step approach. All data are reported with mean  $\pm$  standard deviation (SD). Statistical significance was reported for  $p < 0.05$ .

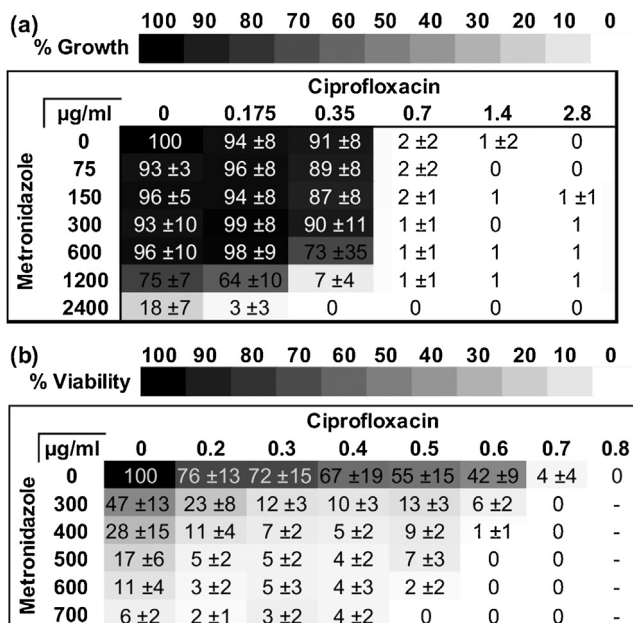


**Fig. 2 – (a) % Growth determined by OD<sub>600nm</sub> readings of bacterial cultures incubated with antibiotics for 18 h at 37°C and 5% CO<sub>2</sub> (n = 9). In a separate experiment, (b) % *S. mutans* viability was determined by CFU counts after sub-culturing the overnight suspension cultures incubated with antibiotics on THYE agar plates. Sub-cultured colonies were counted after 48 h of incubation at 37°C and 5% CO<sub>2</sub> (n = 9).**

## 3. Results

### 3.1. Susceptibility of *S. mutans* to the selected antibiotics

Susceptibility of *S. mutans* to CF and MN was determined with % growth by OD readings (Fig. 2a) and % viability by sub-culturing (Fig. 2b). The MICs for CF and MN were determined to be 0.7 and 2400 µg/mL, respectively. The drug combination (0.35 µg/mL of CF with 1200 µg/mL of MN) had an additive effect (FICI = 1) against *S. mutans*. The minimum bactericidal concentration (MBC) that kills more than 99.9% of the bacterial culture was 0.8 µg/mL for CF (Fig. 2b). The required concentration of CF to reach the MBC threshold decreased with increase in MN concentration.

### 3.2. Synthesis and characterization of HLH-MN

After purification with 1N HCl and water, the yield for coupling MN to the pendent carboxylic acid moiety of HLH was 70–85%, calculated by <sup>1</sup>H-NMR (Supplementary Fig. S2) using peak intensities of C=CH–N from MN (1H,  $\delta = 7.96$  ppm) and trans-CH<sub>2</sub>=C(CH<sub>3</sub>)COO (2H,  $\delta = 6.13$ ) from the methacrylate moiety. HLH-MN was detected by positive mode ESI-MS at  $m/z$  612 [M+H<sup>+</sup>] and 634 [M+Na<sup>+</sup>], with “M” as the given pure entity being analyzed (Supplementary Fig. S2).

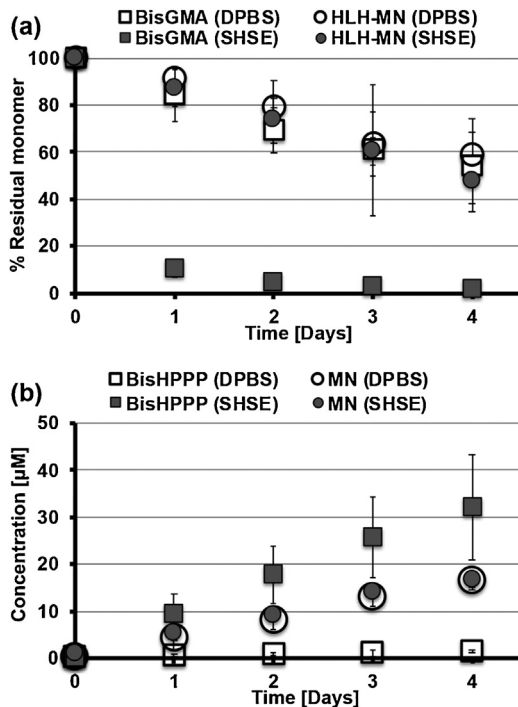


**Fig. 3** – Biodegradation analysis of monomers incubated in solution at 37°C (n = 9). (a) % Residual monomer left in solution and (b) degradation by-products BisHPPP and MN released from BisGMA and HLH-MN, respectively.

### 3.3. Biodegradation analysis

The HLH-MN oligomer was more stable than BisGMA in the presence of esterase activity. Within 48 h of incubation in SHSE, more than 90% of BisGMA had undergone hydrolysis as compared to only ~30% for HLH-MN (Fig. 3a). After 4 days of incubation in SHSE, less than 2% of BisGMA was left in solution as compared to more than 45% of HLH-MN. In buffer however, HLH-MN and BisGMA had similar susceptibilities to hydrolysis with 59% of HLH-MN and 54% of BisGMA left in solution after 4 days of incubation in DPBS. A significantly higher amount of BisHPPP, terminal degradation by-product from BisGMA, was released when incubated in SHSE as compared to when incubated in DPBS (Fig. 3b). The amount of MN released from the HLH-MN oligomer however was not significantly different between the buffer and enzyme condition. Esterase activity also did not increase the cumulative release of MN from films (supplementary Fig. S3). Furthermore, HLH-MN when added to polymerized films, was not found to alter the susceptibility of the BisGMA component to hydrolysis.

### 3.4. Cytotoxicity

HGFs seeded over films containing the antimicrobial oligomers (HLH-CFPEG or HLH-MN) were found to be metabolically active, as measured by the WST-1 assay, with no significant difference in the % cellularity (measured DNA content as a percentage of the growth media control) when compared to the in-house control (0:0:55:45) prepared from BisGMA and HEMA (Fig. 4). This was observed in both

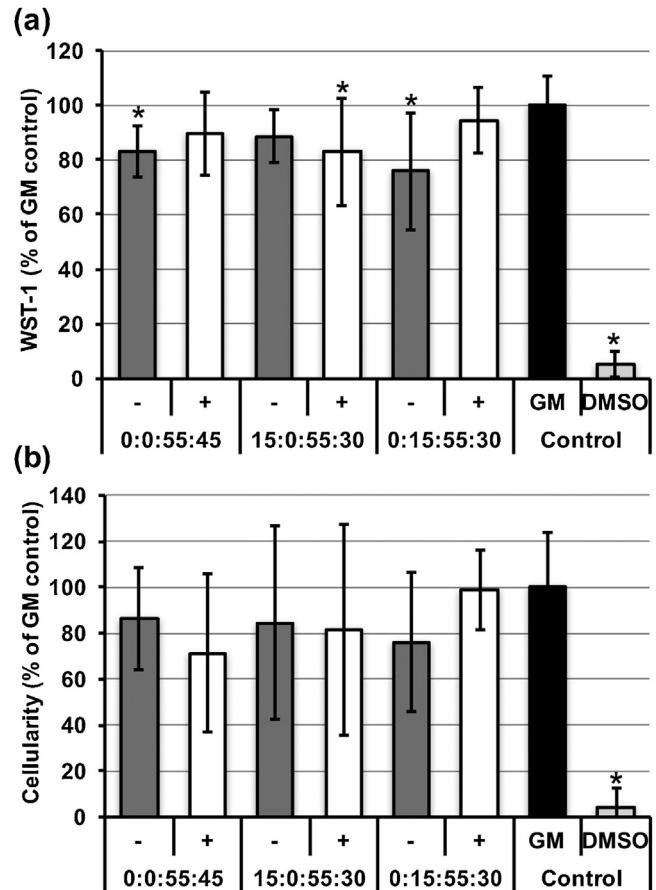


**Fig. 4** – Cytotoxicity of films with (+) and without (–) residual monomer. (a) WST-1 and (b) % Cellular DNA normalized to growth media (GM) control (n = 11). \*Denotes significant difference ( $p < 0.05$ ) from GM control.

conditions, with and without residual unreacted oligomers extracted. Films incubated with HGFs showed a small drop in WST readings relative to the no film control.

The concentration of resin by-product extracts from cured resins in the 28-day DMEM incubated solutions were determined by HPLC. The MAA concentration from the following formulations 0:0:55:45, 15:0:55:30, 0:15:55:30 were  $5.66 \pm 1.58 \mu\text{g/mL}$ ,  $3.54 \pm 1.55 \mu\text{g/mL}$ ,  $4.54 \pm 2.28 \mu\text{g/mL}$ , respectively. For the aforementioned formulations, the concentration of BisHPPP was  $2.27 \pm 1.13 \mu\text{g/mL}$ ,  $3.76 \pm 2.37 \mu\text{g/mL}$ , and  $1.01 \pm 0.25 \mu\text{g/mL}$ , respectively. The antimicrobial formulation 15:0:55:30 had accumulated  $0.04 \pm 0.01 \mu\text{g/mL}$  of CF and the 0:15:55:30 formulation had accumulated  $0.33 \pm 0.07 \mu\text{g/mL}$  of MN. At these given concentrations, the DMEM extracts did not pose a cytotoxic effect to HGFs, given that no significant differences were observed in the % cellularity and metabolic activity for cultures incubated with the 28-day DMEM extract test solutions when compared to the media control (Fig. 5).

### 3.5. Physical characterization

The degree of swelling in water was significantly less in 0:15:55:30, 15:15:55:15, and 20:15:55:10 when compared to 0:0:55:45 (Table 1). Reducing HEMA content also significantly

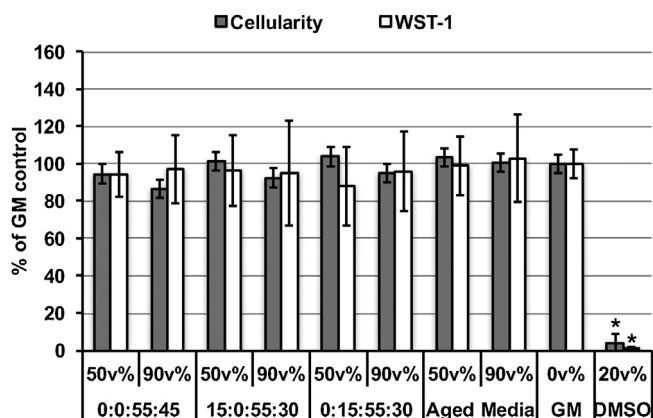


**Fig. 5 – Cytotoxicity assessment of DMEM extracted by-products (n=9). \*Denotes significant difference (p < 0.05) from growth media control.**

reduced the % gel content achieved in the highest antimicrobial formulation (20:15:55:10). All cured films had advancing water contact angles of approximately 74–78°, and receding angles of 54–55°. The resin formulation with the highest drug oligomer content (20:15:55:10) had an advancing contact angle value significantly higher (p < 0.05) than the control (0:0:55:45), but no significant difference was observed for the remaining formulations when compared to the in-house control (0:0:55:45).

Both HLH-CFPEG and HLH-MN are miscible with HEMA, and soluble in common organic solvents such as ethanol, acetone, and tetrahydrofuran. At 25°C, BisGMA and HLH-MN had a Newtonian behavior but HLH-CFPEG presented a non-Newtonian behavior with progressive shear thinning (Fig. 6a) as the viscosity decreased with an increase in shear rates (Fig. 6b). Both oligomers have a lower viscosity when compared to the commercial monomer BisGMA (Fig. 6b).

All adhesive formulations (containing 13.8 wt% ethanol) exhibited a Newtonian behavior with viscosities independent of the applied shear rate between 6–600 s<sup>-1</sup> (Fig. 7). Viscosities reported in Table 1 were calculated by taking the average viscosity value in the plateau region for each formulation. The

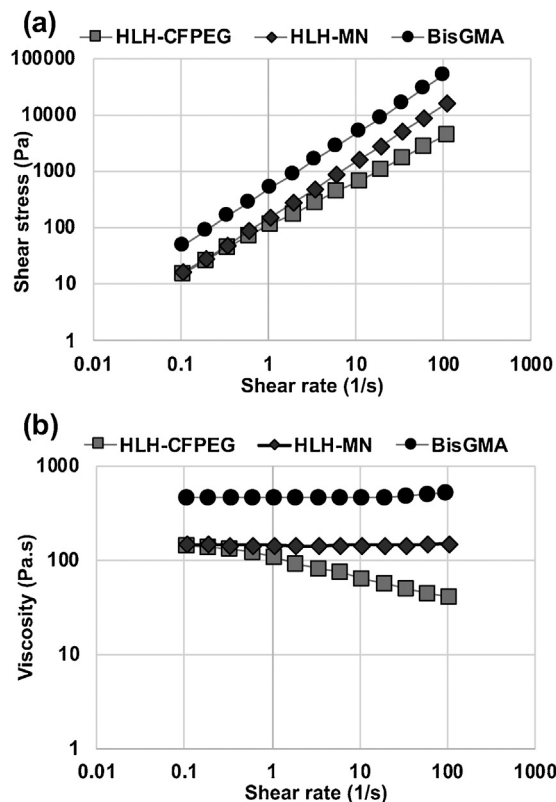


**Fig. 6 – (a) Shear stress versus shear rate, and (b) shear viscosity versus shear rate for the three monomers HLH-CFPEG, HLH-MN, and BisGMA.**

viscosities for the drug oligomer containing adhesives were between 2 and 10-times higher than the control (0:0:55:45) depending on the amount of drug oligomer and diluent HEMA in the formulated mixture (Table 1).

**3.6. Interfacial fracture toughness**

The formulated experimental adhesives demonstrated bonding to dentin in both 2-step and 3-step applications. In

**Table 1 – Viscosity of the formulated adhesives were determined using a rheometer. Solvent evaporation during light curing (n = 12), gel content (n = 9), and degree of water swelling (n = 12) were measured by gravimetric analysis. Water contact angles (n = 15) were measured by means of a goniometer on films that were air-dried for 15 min prior to light curing.**

Composition	Formulated adhesives (containing 13.8 wt% ethanol)				Cured films (air-dried prior curing)		
	Viscosity (Pa.s)	Solvent evaporation during curing (wt %)	Gel content (wt %)	Water Swelling (wt %)	Contact angle (°)		
					Advancing	Receding	Hysteresis
0:0:55:45 (rel. control)	0.05	5.2 ± 1.2	99.4 ± 1.1	8.2 ± 0.7	75 ± 3	55 ± 6	20
15:0:55:30	0.11	3.7 ± 1.5	97.0 ± 3.5	7.2 ± 0.8	74 ± 2	54 ± 4	21
0:15:55:30	0.13	3.1 ± 1.4*	96.8 ± 1.9	6.4 ± 0.9*	74 ± 2	54 ± 4	21
15:15:55:15	0.31	2.6 ± 1.1*	97.8 ± 2.3	5.6 ± 1.5*	76 ± 1	54 ± 4	21
20:15:55:10	0.66	3.1 ± 1.8*	93.9 ± 1.6*	4.9 ± 0.5*	78 ± 2*	55 ± 4	24

\* Denotes significant difference (p < 0.05) from control (0:0:55:45).

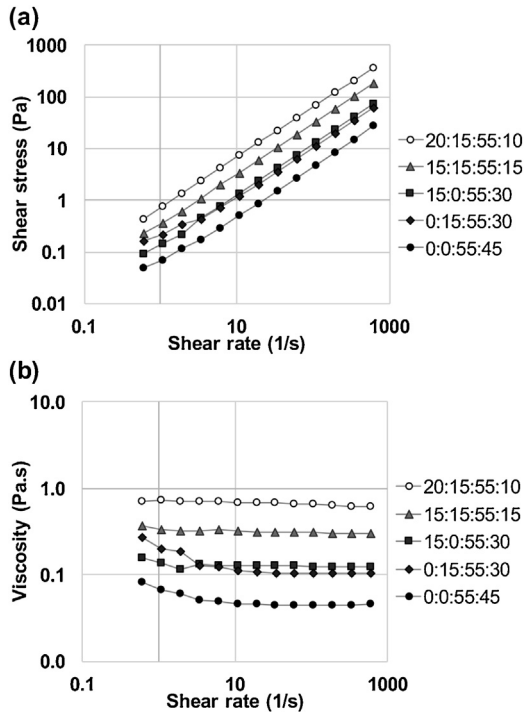


Fig. 7 – (a) Shear stress versus shear rate, and (b) shear viscosity versus shear rate for the formulated adhesives containing ethanol and photo-initiators.

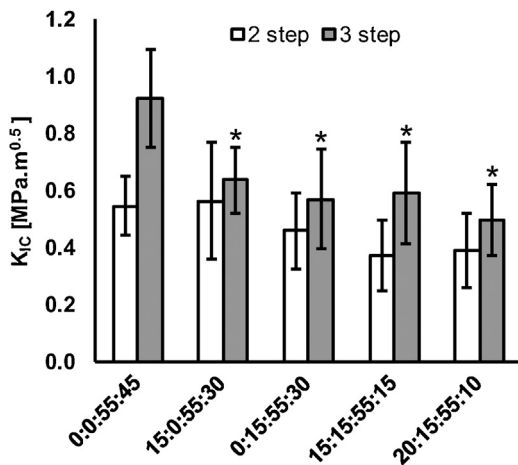


Fig. 8 – Fracture toughness analysis of the restoration-dentin interface with 2-step and 3-step application for  $n = 10$ , except for 15:0:55:30 (2-step) which had  $n = 9$ . \*Denotes significant difference ( $p < 0.05$ ) from the control formulation (0:0:55:45).

the 2-step application technique,  $K_{IC}$  values for the control (0:0:55:45) were not significantly different from drug oligomer containing formulations (Fig. 8). In the 3-step adhesive application,  $K_{IC}$  for the control (0:0:55:45) were statistically higher than all test groups. All samples predominantly failed along the dentin-bonded interface (Fig. 9).

The SEM images of the fractured surfaces illustrated well-developed resin tags in all formulated adhesives, both in the

2-step application (Fig. 9) and 3-step approach (Fig. 10). No significant difference was seen in the % of filled tubules on the dentin surfaces of the antimicrobial formulations versus control (0:0:55:45), in both the 2-step (Fig. 9) and 3-step (Fig. 10) approach. The 3-step application had a significantly greater % of dentinal tubules filled with resin post fracture when compared to the 2-step approach for all adhesives except 0:15:55:30.

#### 4. Discussion

Biofilm derived bacteria existing within the dentin-restoration interface are a major contributing factor to secondary caries. They can promote demineralization of the adjacent dentin and participate in the degradation of the resin at the interface [8–10]. Local delivery by means of hydrolytic release at the surface of restorative adhesive materials within the marginal gap is thus an attractive approach to counter bacteria. CF was selected as a model agent due to its low MIC (0.7  $\mu\text{g/mL}$ ) and MBC (0.8  $\mu\text{g/mL}$ ) against *S. mutans* (Fig. 2), an etiological agent of dental caries [31]. The values for CF are about two-orders of magnitude lower than many other commonly used agents such as chlorhexidine digluconate (MIC of 70  $\mu\text{g/mL}$  and MBC of 150  $\mu\text{g/mL}$ ) [32] and epigallocatechin gallate (MIC of 31.25  $\mu\text{g/mL}$  and MBC of 62.5  $\mu\text{g/mL}$ ) [33]. Although the MIC of MN was greater, the combination with CF presented an additive effect against *S. mutans*. Since CF and MN have different modes of action [34], the combination broadens the spectrum of activity and potentially reduces the likelihood of developing resistant bacterial strains [17].

Upon hydrolytic degradation of the drug oligomers, CF and MN were released from HLH-CFPEG [18] and HLH-MN (Fig. 3a), respectively. Both oligomers presented greater stability against esterolytic degradation when compared to the commercial monomer BisGMA. As anticipated based on the literature for resin biodegradation by CE [19], a significantly higher amount of BisHPPP was released when BisGMA was incubated in SHSE as compared to when incubated in DPBS (Fig. 3b). After 2 days of incubation in SHSE, less than 5% residual BisGMA was left in solution while more than 70% residual oligomers of HLH-MN (Fig. 3a) and HLH-CFPEG [18] were detected. The relative resistance of the antimicrobial oligomers to esterase activity compared to BisGMA may be related to substrate preference for CE [35] and/or the unhindered esters in BisGMA vs. steric hindrance afforded by the branched structure in the antimicrobial oligomers. Hydrogen bonding provided by the urethane chemistry in the dimethacrylate backbone may also contribute to the improved resistance by influencing the manner in which the enzymes adsorb, bind and interact with the substrate [19].

The hydrophilic nature of the films is mediated by polar functional groups such as ethers, urethanes, carbonyls and hydroxyls. The greater water uptake by the 0:0:55:45 formulation is thought to be related to the polymer having more moles of polar moieties (i.e. hydroxyl functionality in HEMA), when compared to the antimicrobial formulations. The drug oligomers, although more hydrophobic than HEMA, still contain several polar groups that can attract and interact with water molecules. Water uptake makes the polymer's hydrolyt-

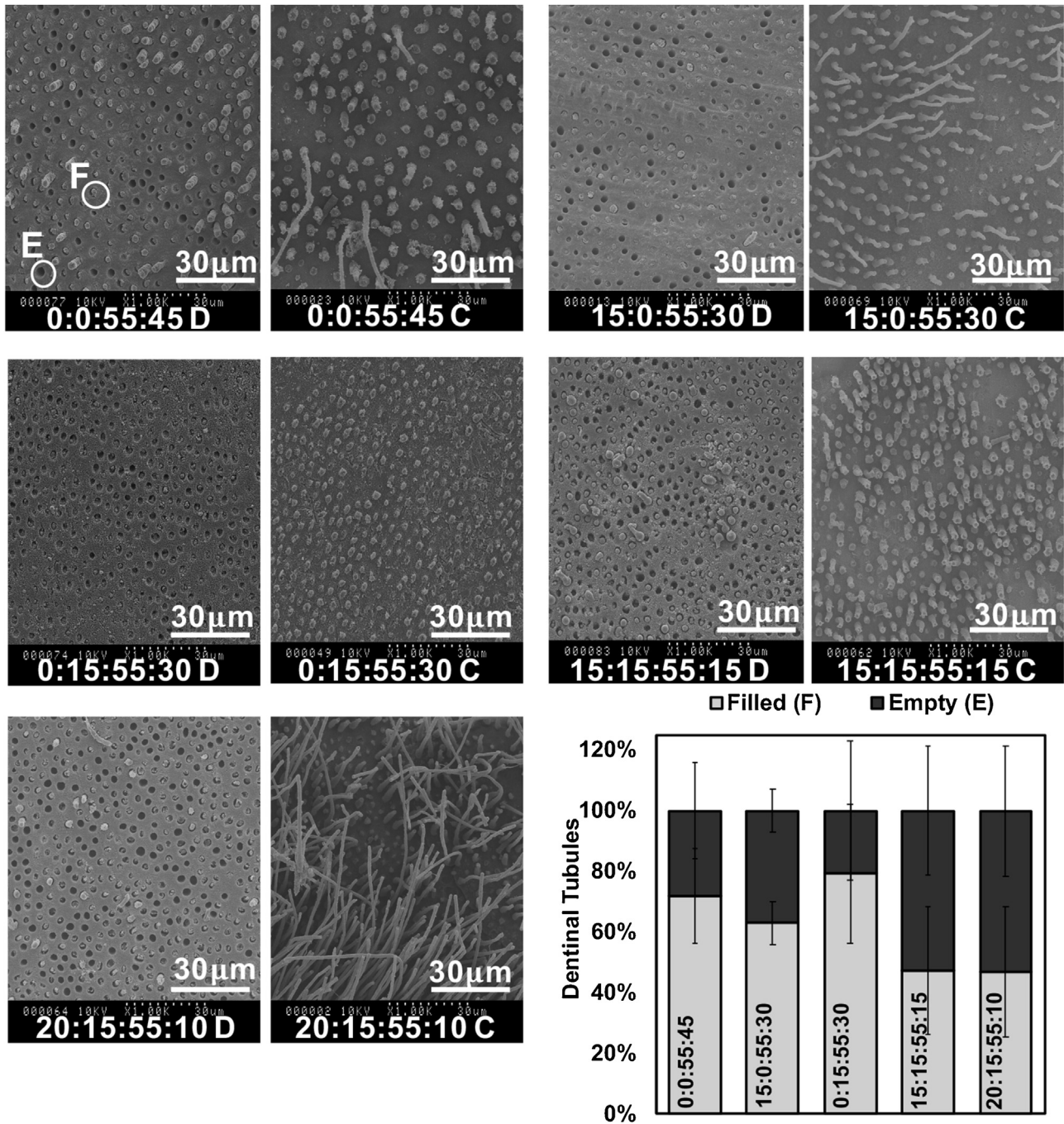


**Fig. 9** – Fractography analysis of the restoration-dentin interface with 2-step application was performed by SEM on the dentin surface (D) and opposing composite surface (C). The number of dentinal tubules on the dentin surface were counted. The percentage of empty (E) tubules (dark core) and tubules filled (F) with resin (white core) were calculated per image (n = 5–6).

ically sensitive group’s more prone to hydrolysis. Swelling by water uptake also facilitates leaching of residual methacrylate monomers [36], which are cytotoxic [37]. Larger and bulkier monomers generally leach out slower [38], while hydrophilic small molecules such as HEMA leach out more rapidly [39]. Therefore, HEMA was replaced with the drug oligomers in the antimicrobial formulations. The polymerized formulations containing the antimicrobial oligomers presented no

cytotoxic concerns against HGFs. In a number of films seeded with HGFs, a small drop in WST-1 was observed (Fig. 4a). These small variances were considered as having no practical significance since the DNA values presented no changes (Fig. 4b). Further, based on ISO 10993-5, these materials are considered non-cytotoxic as the metabolic activity and % cellularity was above 70% of the GM control for all tested samples.

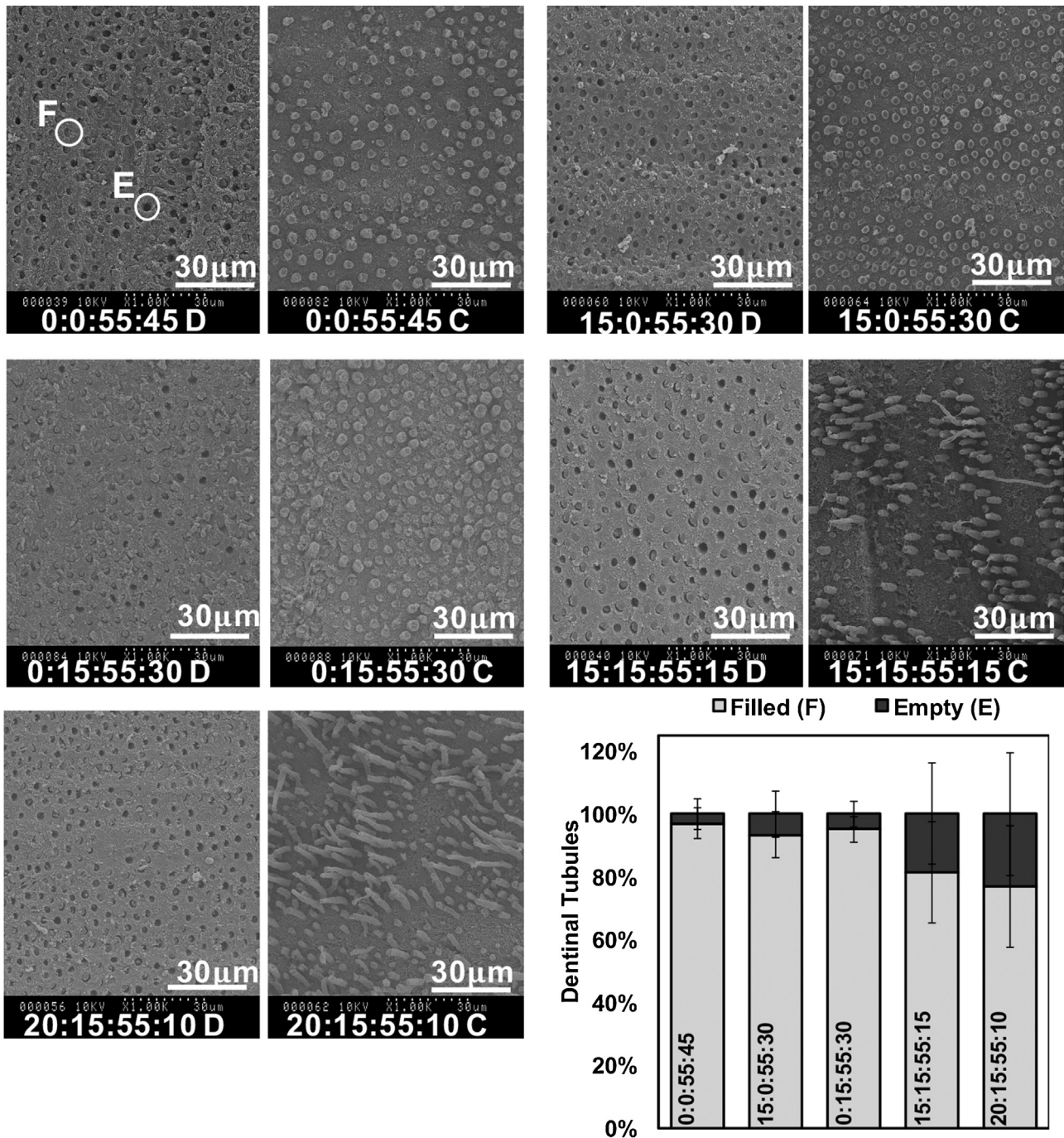


**Fig. 10** – Fractography analysis of the restoration-dentin interface with 3-step application was performed by SEM on the dentin surface (D) and opposing composite surface (C). The number of dentinal tubules on the dentin surface were counted. The percentage of empty (E) tubules (dark core) and tubules filled (F) with resin (white core) were calculated per image (n = 6).

The viscosity of the adhesive solution is an important practical parameter, as it influences spreading on the tooth substrate [40], resin infiltration [41], and polymerization. HEMA is incorporated into the bonding systems to reduce viscosity, aid with homogenous mixing of hydrophobic and hydrophilic monomers [2], and help promote the diffusion of co-monomers into demineralized dentin by expanding the collagen network [42]. However, HEMA is a mono-functional monomer that forms a linear and flexible polymer upon

curing, with inferior mechanical character relative to a crosslinked system [2].

Both drug oligomers are less viscous in comparison to the commercial monomer BisGMA. The high viscosity of BisGMA is attributed to the intermolecular interactions, which includes hydrogen bonding between hydroxyl and carbonyl groups and pi-pi bonding between aromatic groups [43]. BisGMA and HLH-MN presented a Newtonian behavior at the studied shear rates, holding a linear relationship between

shear stress and shear rate, with viscosity as the constant of proportionality. HLH-CFPEG presented a non-Newtonian behavior with progressive shear thinning, with viscosity decreasing as shear rates increase. Shear thinning arises from a decrease in resistance to flow, caused by molecules orienting with the applied shear force (commonly seen with polymers) [44], or the disruption in intermolecular interactions (i.e. hydrogen bonding) by the applied shear force [45]. Shear thinning in HLH-CFPEG is believed to be primarily arising from the higher molecular weight chains of the conjugated PEG. It should be noted that BisGMA has also been reported to undergo shear thinning, but at higher shear rates (approximately  $>100\text{ s}^{-1}$ ) in which the hydrogen bonded networks are interrupted and the number of inter-chain bonds are reduced, thus lowering the resistance to flow and consequently reducing the viscosity [45].

The experimental adhesives presented a Newtonian behavior with much lower viscosities (0.05–0.66 Pa·s) than the pure monomer forms. The lower viscosities can be attributed to the solvent (i.e. ethanol) disrupting intermolecular forces. The viscosities of the experimental adhesives are on the order of magnitude reported for commercial systems. For example, Scotchbond Multi-Purpose adhesive (3M ESPE, St. Paul, MN, USA), which is used in a 3-step E&R system, has been reported to have a viscosity of 0.38 Pa·s [46]. Prime & Bond NT (DENTSPLY De Trey, Konstanz, Germany) used in 2-step E&R applications has a viscosity of 0.0014 Pa·s [47]. Replacing HEMA with the drug oligomers increased viscosity in the experimental adhesive solutions. Both drug oligomers have a higher molecular weight when compared to HEMA in addition to having polar linkages such as urethanes and esters that can participate in hydrogen bonding. Inter- and intra-molecular interactions increase viscosity [43]. CF is also known to aggregate due to strong pi-pi bonding between the aromatic groups that causes the CF molecules to stack in aqueous solutions [48]. The higher viscosity of the antimicrobial adhesives when compared to the in-house control did not appear to influence resin infiltration into the dentinal tubules (Fig. 9). Filled tubules and/or resin tags attached to the composite surface were observed post fracture with all formulations studied. The fractured resin tags at the dentin surface are an indication of good penetration and interaction with dentin, a potential contributing element to an effective mechanical bond. A greater number of longer resin tags attached to the opposing composite surface was observed in the formulation containing the highest wt% of antimicrobial drugs (20:15:55:10), in both the 2-step and 3-step application. This suggest that resin infiltration is occurring, but that the resin is forming weaker interactions with the tooth substrate. The use of a primer (containing water and HEMA) can influence resin interaction with dentin, by lowering viscosity and providing hydrophilic character to penetrate and interact with the hydrophilic dentin substrate [42]. For all studied formulations except 0:15:55:30, a significantly greater percentage of filled tubules were observed on the fractured surfaces in the 3-step application as compared to the 2-step approach. For 0:0:55:45, application of the primer also increased  $K_{IC}$  values, however a significant increase was not observed in the drug oligomer containing formulations. The role of effective resin infiltration and its influence on fracture toughness is still an unclear topic of much debate in the den-

tal literature. Several studies have shown a lack of correlation between resin infiltration and hybridization with interfacial fracture toughness or bond strength [49,50].

The  $K_{IC}$  values obtained for both the 2-step and 3-step application of the experimental adhesives were within the range of values reported for commercial products (0.2–1.2 MPa·m<sup>0.5</sup>) [51]. The magnitude of  $K_{IC}$  represents the critical stress intensity around a propagating crack triggered by mode-I (tensile force) failure, which gives rise to an inherent material property [51]. Testing using mini-SR specimens results in the fracture predominantly occurring along the resin–dentin interface, and thus the obtained interfacial fracture toughness values provide results on the intrinsic properties of the material in response to a clinically relevant failure [29,50].

The slightly lower  $K_{IC}$  values for the antimicrobial formulations containing the drug oligomers may be a result of solvent (ethanol) retention post curing. Ethanol plays an important role during bonding as it displaces water from the collagen networks and allows for the monomers to infiltrate into the wet dentin. Ethanol also reduces viscosity which improves diffusivity [2]. Residual solvent post curing can result in a porous structure that compromises the structural integrity of the marginal seal [52]. A lower ultimate tensile strength and modulus of elasticity was observed at higher ethanol concentrations, when BisGMA and HEMA (60:40 wt%) were cured in the presence of ethanol [53]. The extent of ethanol retention depends on the adhesive polarity and capacity to hydrogen bond with the co-monomers [54], and the molar concentrations of the different co-monomers in the adhesive [55]. Increasing the concentration of drug oligomers was found to significantly reduce the wt% of solvent evaporated during 20 s of light curing (Table 1). This suggests that greater residual solvent is expected post curing in samples containing higher wt% of drug oligomers. Replacing HEMA with HLH-CFPEG and HLH-MN appears to cause solvent retention in the adhesive during curing as the drug oligomers introduce polar character associated with the urethane linkages that can hydrogen bond with ethanol, and water in the primer used in the 3-step application [54]. Gel content, which is a relative proxy for the degree of monomer incorporation into the polymer matrix [56], was slightly lower with the 20:15:55:10 formulation containing the greatest wt% of drug oligomers (Table 1). This may be a result of slower evaporation of ethanol and/or the higher viscosity in the unreacted antimicrobial solution. Therefore, further optimization of monomer and solvent ratios, wt% of initiator used, curing time, and air stream may improve interfacial fracture toughness values.

Biodegradation of the resin can deteriorate mechanical integrity of the interface over time, as previous studies have shown a decrease in interfacial  $K_{IC}$  after 6 months of exposure to esterase activities for E&R systems [6,30]. Both drug oligomers are hydrolytically more stable against enzyme catalyzed degradation in comparison to BisGMA, which may further address the time-dependent decrease in interfacial  $K_{IC}$  with esterase exposure for current commercial resins [6,30]. Upon release of antibiotics, there is also a possibility for ionic bonding to occur between the generated carboxylic acid functional groups on the dimethacrylate backbone and the cations ( $\text{Ca}^{2+}$ ) in teeth. A mechanism that is used in GIC restorations,

with carboxylate groups on the polyacid molecules ionically bonding to calcium ions (Ca<sup>2+</sup>) in the tooth [57]. Hence, while the mechanical studies undertaken in this study for as-made bonding interfaces are slightly less for the drug formulations than those of the control, longer term studies in aging biodegradation solutions may show significant advantages for the new formulations by retaining and stabilizing the initial bond strength vs. the unstable bond by traditional total etch formulations.

## 5. Conclusion

Bonding to dentin was achieved using formulations containing the antimicrobial oligomers. Incorporating antibiotics into dental adhesive systems using hydrolysable linkages provides a means to delivery antibiotics at the margins of the tooth and filling material, in order to control bacteria accumulation. The greater stability of the antimicrobial oligomers in the presence of GE may reduce the detrimental effect of enzymatic degradation on interfacial fracture toughness over time. Future work should further optimize the formulation and investigate the effect of long-term incubation in cariogenic environments on K<sub>IC</sub> values.

## Acknowledgements

This research was supported by the Natural Sciences and Engineering Research Council of Canada (NSERC), Discovery grant #360520 and Canada Graduate Scholarship (CGS-D). The authors would like to thank Dr. Muna Marashdeh for her technical assistance, Dr. Jian Wang for his assistance with the Instron testing machine, and Jake Cosme for running the ESI-MS samples.

## Appendix A. Supplementary data

Supplementary data associated with this article can be found, in the online version, at <https://doi.org/10.1016/j.dental.2018.11.016>.

## REFERENCES

- [1] Beazoglou T, Eklund S, Heffley D, Meiers J, Brown LJ, Bailit H. Economic impact of regulating the use of amalgam restorations. *Public Health Rep* 2007;122:657–63.
- [2] Van Landuyt KL, Snauwaert J, De Munck J, Peumans M, Yoshida Y, Poitevin A, et al. Systematic review of the chemical composition of contemporary dental adhesives. *Biomaterials* 2007;28:3757–85, <http://dx.doi.org/10.1016/j.biomaterials.2007.04.044>.
- [3] Owens BM, Johnson WW, Harris EF. Marginal permeability of self-etch and total-etch adhesive systems. *Oper Dent* 2006;31:60–7, <http://dx.doi.org/10.2341/04-185>.
- [4] Cardoso MV, de Almeida Neves A, Mine A, Coutinho E, Van Landuyt K, De Munck J, et al. Current aspects on bonding effectiveness and stability in adhesive dentistry. *Aust Dent J* 2011;56:31–44, <http://dx.doi.org/10.1111/j.1834-7819.2011.01294.x>.
- [5] Pashley DH, Tay FR, Breschi L, Tjäderhane L, Carvalho RM, Carrilho M, et al. State of the art etch-and-rinse adhesives. *Dent Mater* 2011;27:1–16, <http://dx.doi.org/10.1016/j.dental.2010.10.016>.
- [6] Shokati B, Tam LE, Santerre JP, Finer Y. Effect of salivary esterase on the integrity and fracture toughness of the dentin-resin interface. *J Biomed Mater Res B Appl Biomater* 2010;94:230–7, <http://dx.doi.org/10.1002/jbm.b.31645>.
- [7] Kermanshahi S, Santerre JP, Cvitkovitch DG, Finer Y. Biodegradation of resin–dentin interfaces increases bacterial microleakage. *J Dent Res* 2010;89:996–1001, <http://dx.doi.org/10.1177/0022034510372885>.
- [8] Marashdeh MQ, Gitalis R, Levesque C, Finer Y. *Enterococcus faecalis* hydrolyzes dental resin composites and adhesives. *J Endod* 2018;44:609–13, <http://dx.doi.org/10.1016/j.joen.2017.12.014>.
- [9] Huang B, Siqueira WL, Cvitkovitch DG, Finer Y. Esterase from a cariogenic bacterium hydrolyzes dental resins. *Acta Biomater* 2018;71:330–8, <http://dx.doi.org/10.1016/j.actbio.2018.02.020>.
- [10] Bourbia M, Ma D, Cvitkovitch DG, Santerre JP, Finer Y. Cariogenic bacteria degrade dental resin composites and adhesives. *J Dent Res* 2013;92:989–94, <http://dx.doi.org/10.1177/0022034513504436>.
- [11] Eltahlah D, Lynch CD, Chadwick BL, Blum IR, Wilson NHF. An update on the reasons for placement and replacement of direct restorations. *J Dent* 2018;72:1–7, <http://dx.doi.org/10.1016/j.jdent.2018.03.001>.
- [12] Stanislawczuk R, Reis A, Malaquias P, Pereira F, Farago PV, Meier MM, et al. Mechanical properties and modeling of drug release from chlorhexidine-containing etch-and-rinse adhesives. *Dent Mater* 2014;30:392–9, <http://dx.doi.org/10.1016/j.dental.2014.01.007>.
- [13] Kasraei S, Sami L, Hendi S, AliKhani M-Y, Rezaei-Soufi L, Khamverdi Z. Antibacterial properties of composite resins incorporating silver and zinc oxide nanoparticles on *Streptococcus mutans* and *Lactobacillus*. *Restor Dent Endod* 2014;39:109–14, <http://dx.doi.org/10.5395/rde.2014.39.2.109>.
- [14] Yesilyurt C, Er K, Tasdemir T, Buruk K, Celik D. Antibacterial activity and physical properties of glass-ionomer cements containing antibiotics. *Oper Dent* 2009;34:18–23, <http://dx.doi.org/10.2341/08-30>.
- [15] Coates A, Hu Y, Bax R, Page C. The future challenges facing the development of new antimicrobial drugs. *Nat Rev Drug Discov* 2002;1:895–910, <http://dx.doi.org/10.1038/nrd940>.
- [16] Bayramov DF, Neff JA. Beyond conventional antibiotics — new directions for combination products to combat biofilm. *Adv Drug Deliv Rev* 2017;112:48–60, <http://dx.doi.org/10.1016/j.addr.2016.07.010>.
- [17] Soothill G, Hu Y, Coates A. Can we prevent antimicrobial resistance by using antimicrobials better? *Pathogens* 2013;2:422–35, <http://dx.doi.org/10.3390/pathogens2020422>.
- [18] Delaviz Y, Nascimento MA, Laschuk MW, Liu TW, Yang M, Santerre JP. Synthesis and characterization of Ciprofloxacin-containing divinyl oligomers and assessment of their biodegradation in simulated salivary esterase. *Dent Mater* 2018;34:711–25, <http://dx.doi.org/10.1016/j.dental.2018.01.021>.
- [19] Finer Y, Santerre JP. The influence of resin chemistry on a dental composite's biodegradation. *J Biomed Mater Res A* 2004;69:233–46, <http://dx.doi.org/10.1002/jbm.a.30000>.
- [20] Das D, Srinivasan S, Kelly AM, Chiu DY, Daugherty BK, Ratner DM, et al. RAFT polymerization of ciprofloxacin prodrug monomers for the controlled intracellular delivery of antibiotics. *Polym Chem* 2016;7:826–37, <http://dx.doi.org/10.1039/c5py01704a>.
- [21] Kenawy E, Al-deyab SS, Shaker NO, El-sadek BM, Khatbab AHB. Synthesis and antimicrobial activity of metronidazole

- containing polymer and copolymers. *J Appl Polym Sci* 2009;113:818–26, <http://dx.doi.org/10.1002/app.29814>.
- [22] Goc A, Niedzwiecki A, Rath M. Cooperation of doxycycline with phytochemicals and micronutrients against active and persistent forms of *Borrelia* sp. *Int J Biol Sci* 2016;12:1093–103, <http://dx.doi.org/10.7150/ijbs.16060>.
- [23] Cha J-D, Jung E-K, Choi S-M, Lee K-Y, Kang S-W. Antimicrobial activity of the chloroform fraction of *Drynaria fortunei* against oral pathogens. *J Oral Sci* 2017;59:31–8, <http://dx.doi.org/10.2334/josnusd.16-0150>.
- [24] Cai K, Delaviz Y, Banh M, Guo Y, Santerre JP. Biodegradation of composite resin with ester linkages: identifying human salivary enzyme activity with a potential role in the esterolytic process. *Dent Mater* 2014;30:848–60, <http://dx.doi.org/10.1016/j.dental.2014.05.031>.
- [25] Moharamzadeh K, Van Noort R, Brook IM, Scutt AM. Cytotoxicity of resin monomers on human gingival fibroblasts and HaCaT keratinocytes. *Dent Mater* 2007;23:40–4, <http://dx.doi.org/10.1016/j.dental.2005.11.039>.
- [26] Battiston KG, Labow RS, Santerre JP. Protein binding mediation of biomaterial-dependent monocyte activation on a degradable polar hydrophobic ionic polyurethane. *Biomaterials* 2012;33:8316–28, <http://dx.doi.org/10.1016/j.biomaterials.2012.08.014>.
- [27] Wright MEE, Wong AT, Levitt D, Parrag IC, Yang M, Santerre JP. Influence of ciprofloxacin-based additives on the hydrolysis of nanofiber polyurethane membranes. *J Biomed Mater Res A* 2018;106:1211–22, <http://dx.doi.org/10.1002/jbm.a.36318>.
- [28] Park J, Ye Q, Topp E, Misra A, Kieweg SL, Spencer P. Effect of photoinitiator system and water content on dynamic mechanical properties of a light-cured bisGMA/HEMA dental resin. *J Biomed Mater Res A* 2010;93:1245–51, <http://dx.doi.org/10.1002/jbm.a.32617>.
- [29] Tam LE, Pilliar RM. Fracture toughness of dentin/resin-composite adhesive interfaces. *J Dent Res* 1993;72:953–9 <https://doi.org/10.1177/00220345930720051801>.
- [30] Serkies KB, Garcha R, Tam LE, De Souza GM, Finer Y. Matrix metalloproteinase inhibitor modulates esterase-catalyzed degradation of resin–dentin interfaces. *Dent Mater* 2016;32:1513–23, <http://dx.doi.org/10.1016/j.dental.2016.09.007>.
- [31] Lenander-Lumikari M, Loimaranta V. Saliva and dental caries. *Adv Dent Res* 2000;14:40–7, <http://dx.doi.org/10.1177/08959374000140010601>.
- [32] Uzer Celik E, Tunac AT, Ates M, Sen BH. Antimicrobial activity of different disinfectants against cariogenic microorganisms. *Braz Oral Res* 2016;30:e125, <http://dx.doi.org/10.1590/1807-3107BOR-2016.vol30.0125>.
- [33] Xu X, Zhou XD, Wu CD. The tea catechin epigallocatechin gallate suppresses cariogenic virulence factors of *Streptococcus mutans*. *Antimicrob Agents Chemother* 2011;55:1229–36, <http://dx.doi.org/10.1128/AAC.01016-10>.
- [34] Windley W, Teixeira F, Levin L, Sigurdsson A, Trope M. Disinfection of immature teeth with a triple antibiotic paste. *J Endod* 2005;31:439–43 <https://doi.org/10.1097/01.don.0000148143.80283.ea>.
- [35] Lin BA, Jaffer F, Duff MD, Tang YW, Santerre JP. Identifying enzyme activities within human saliva which are relevant to dental resin composite biodegradation. *Biomaterials* 2005;26:4259–64, <http://dx.doi.org/10.1016/j.biomaterials.2004.11.001>.
- [36] Ferracane JL. Hygroscopic and hydrolytic effects in dental polymer networks. *Dent Mater* 2006;22:211–22, <http://dx.doi.org/10.1016/j.dental.2005.05.005>.
- [37] Kaga M, Noda M, Ferracane JL, Nakamura W, Oguchi H, Sano H. The in vitro cytotoxicity of eluates from dentin bonding resins and their effect on tyrosine phosphorylation of L929 cells. *Dent Mater* 2001;17:333–9, [http://dx.doi.org/10.1016/S0109-5641\(00\)00091-9](http://dx.doi.org/10.1016/S0109-5641(00)00091-9).
- [38] Tabatabaei MH, Sadrai S, Bassir SH, Veisy N, Dehghan S. Effect of food stimulated liquids and thermocycling on the monomer elution from a nanofilled composite. *Open Dent J* 2013;7:62–7, <http://dx.doi.org/10.2174/1874210601307010062>.
- [39] Bakopoulou A, Papadopoulos T, Garefis P. Molecular toxicology of substances released from resin-based dental restorative materials. *Int J Mol Sci* 2009;10:3861–99, <http://dx.doi.org/10.3390/ijms10093861>.
- [40] Lee JH, Um CM, Lee IB. Rheological properties of resin composites according to variations in monomer and filler composition. *Dent Mater* 2006;22:515–26, <http://dx.doi.org/10.1016/j.dental.2005.05.008>.
- [41] Irinoda Y, Matsumura Y, Kito H, Nakano T, Toyama T, Nakagaki H, et al. Effect of sealant viscosity on the penetration of resin into human enamel. *Oper Dent* 2000;25:274–82.
- [42] Nakaoki Y, Nikaido T, Pereira PNR, Inokoshi S, Tagami J. Dimensional changes of demineralized dentin treated with HEMA primers. *Dent Mater* 2000;16:441–6, [http://dx.doi.org/10.1016/S0109-5641\(00\)00042-7](http://dx.doi.org/10.1016/S0109-5641(00)00042-7).
- [43] Stansbury JW. Dimethacrylate network formation and polymer property evolution as determined by the selection of monomers and curing conditions. *Dent Mater* 2012;28:13–22, <http://dx.doi.org/10.1016/j.dental.2011.09.005>.
- [44] Förster S, Konrad M, Lindner P. Shear thinning and orientational ordering of Wormlike Micelles. *Phys Rev Lett* 2005;94:14–7, <http://dx.doi.org/10.1103/PhysRevLett.94.017803>.
- [45] Kim JW, Kim LU, Kim CK, Cho BH, Kim OY. Characteristics of novel dental composites containing 2,2-bis[4-(2-methoxy-3-methacryloyloxy propoxy) phenyl] propane as a base resin. *Biomacromolecules* 2006;7:154–60 <https://pubs.acs.org/doi/abs/10.1021/bm0504911>.
- [46] Park ES, Kim CK, Bae JH, Cho BH. The effect of the strength and wetting characteristics of Bis-GMA/TEGDMA-based adhesives on the bond strength to dentin. *J Korean Acad Conserv Dent* 2011;36:139–48 <https://doi.org/10.5395/JKACD.2011.36.2.139>.
- [47] Leforestier E, Darque-Ceretti E, Peiti Ch, Bouchard P-O, Bolla M. Determining the initial viscosity of 4 dental adhesives. Relationship with their penetration into tubuli. *Int J Adhes Adhes* 2010;30:393–402, <http://dx.doi.org/10.1016/j.ijadhadh.2010.02.003>.
- [48] Turcu I, Bogdan M. Size dependence of molecular self-assembling in stacked aggregates. 1. NMR investigation of ciprofloxacin self-association. *J Phys Chem B* 2012;116:6488–98, <http://dx.doi.org/10.1021/jp3034215>.
- [49] Prati C, Chersoni S, Mongiorgi R, Pashley DH. Resin-infiltrated dentin layer formation of new bonding systems. *Oper Dent* 1998;23:185–94.
- [50] Walshaw PR, Tam LE, McComb D. Bond failure at dentin-composite interfaces with 'single-bottle' adhesives. *J Dent* 2003;31:117–25, [http://dx.doi.org/10.1016/S0300-5712\(03\)00007-1](http://dx.doi.org/10.1016/S0300-5712(03)00007-1).
- [51] Soderholm KJ. Review of the fracture toughness approach. *Dent Mater* 2010;26:e63–77, <http://dx.doi.org/10.1016/j.dental.2009.11.151>.
- [52] Tay FR, Gwinnett AJ, Pang KM, Wei SHY. Variability in microleakage observed in a total-etch wet-bonding technique under different handling conditions. *J Dent Res* 1995;74:1168–78, <http://dx.doi.org/10.1177/00220345950740050501>.
- [53] Ye Q, Spencer P, Wang Y, Misra A. Relationship of solvent to the photopolymerization process, properties, and structure in model dentin adhesives. *J Biomed Mater Res* 2007;80:342–50, <http://dx.doi.org/10.1002/jbm.a.30890>.

- 
- [54] Yiu CKY, Pashley EL, Hiraishi N, King NM, Goracci C, Ferrari M, et al. Solvent and water retention in dental adhesive blends after evaporation. *Biomaterials* 2005;26:6863–72, <http://dx.doi.org/10.1016/j.biomaterials.2005.05.011>.
- [55] Cadenaro M, Breschi L, Rueggeberg FA, Suchko M, Grodin E, Agee K, et al. Effects of residual ethanol on the rate and degree of conversion of five experimental resins. *Dent Mater* 2009;25:621–8, <http://dx.doi.org/10.1016/j.dental.2008.11.005>.
- [56] Stansbury JW, Dickens SH. Network formation and compositional drift during photo-initiated copolymerization of dimethacrylate monomers. *Polymer* 2001;42:6363–9, [http://dx.doi.org/10.1016/S0032-3861\(01\)00106-9](http://dx.doi.org/10.1016/S0032-3861(01)00106-9).
- [57] Van Meerbeek B, Yoshida Y, Inoue S, De Munck J, van Landuyt K, Lambrechts P. Glass-ionomer adhesion: the mechanisms at the interface. *J Dent* 2006;34:615–7.